

# Computational Modeling of Spine and Trunk Muscles Subjected to Follower Force

Yoon Hyuk Kim<sup>a,\*</sup>, Kyungsoo Kim<sup>b</sup>

<sup>a</sup>*School of Advanced Technology and Industrial Liaison Research Institute,  
Kyung Hee University, Yongin-si, Gyeonggi-do 449-701, Korea*

<sup>b</sup>*National Institute for Mathematical Sciences, Daejeon 305-333, Korea,  
and Institute of Natural Sciences, Kyung Hee University, Yongin-si, Gyeonggi-do 449-701, Korea*

(Manuscript Received June 5, 2006; Revised January 5, 2007; Accepted January 25, 2007)

---

## Abstract

Recently, the follower force concept was introduced in the field of biomechanics to elucidate how the stability of the human spine could be maintained under substantial compressive loads. However, it has been controversial if the follower load concept is feasible to maintain the spinal stability by coordinating the appropriate trunk muscles. The purpose of this paper is to propose a computational model of the human spine and trunk muscles based on finite element method combining with an optimization formulation subjected to the follower force constraint in order to confirm that the follower force is related to the spinal stability and can be generated by the activation of trunk muscles. Spinal motion segments were modeled as linear elastic beam elements and trunk muscles were assumed to be static. In the optimization formulation, the muscle forces, the follower forces and shear forces, and the deformed shape of the spine model were investigated minimizing the sum of the magnitudes of follower forces under the constraints for the equilibrium equations, the directions of resultant forces, and the physiological bounds of muscle forces. Through a numerical example, it was confirmed that there was a combination of muscle activations transmitting external forces and moments along the follower force direction and the spinal stability was maintained with little change of spinal shape.

*Keywords:* Follower force; Spinal stability; Finite element method; Optimization; Biomechanics

---

## 1. Introduction

Since the 1950s, the importance of stability problem of columns subjected to a tangential follower force has increased in mechanical and aerospace engineering fields. A follower force is a compressive force along a direction tangential to the deflection curve of the column while a non-follower force, or a vertical force, is usually regarded as an axial force preserving its direction constant during the deformation of a structure. The follower force is naturally produced by jet and rocket motors, cantilevered pipes

conveying fluid, dry friction in automotive disk and drum brake systems, and so on (Ryu et al., 1998; Langthjem and Sugiyama, 2000; Wang, 2003). Several studies have presented that the stability of a column subjected to a follower force is increased compared with that subjected to a vertical force (Ryu et al., 1998; Langthjem and Sugiyama, 2000; Wang, 2003; Beck, 1952; Pflüger, 1955; Leipholz, 1980).

Recently, the follower force concept was introduced in the field of biomechanics to elucidate how the stability of the human spine could be maintained under substantial compressive loads during activities of daily life. Patwardhan et al. (1999) developed a new experimental technique for transmitting compressive loads applied at each vertebra to the lower

---

\*Corresponding author. Tel.: +82 31 201 2028; Fax.: +82 31 202 8106  
E-mail address: yoonhkim@khu.ac.kr

vertebra along the follower force direction. They showed that the load-carrying capacity of the spine was significantly increased with slight changes of the spinal shape when compressive loads were carried along the follower force direction at all vertebrae in comparison with the non-follower force direction. There have been several experimental and computational studies supporting the follower force concept (Patwardhan et al., 2000; Patwardhan et al., 2001; Rohlmann et al., 2001; Patwardhan et al., 2001). However, the experimental measurement of muscle contraction forces is difficult and complicated. In addition, to our knowledge, there have been few studies to numerically quantify the role of trunk muscles in the spinal stability based on the follower force concept. Therefore, a computational model of the musculoskeletal system in the human spine could be useful to verify the quantitative role of trunk muscles in spinal stability under the follower force constraint. In this paper, a finite element model of the human spine and trunk muscles was developed and an optimization problem subjected to the follower force constraint was formulated in order to confirm the above hypothesis that the follower force is related to spinal stability and can be generated by the activation of trunk muscles. A two-dimensional numerical example of the lumbar spine was analyzed to verify the presented musculoskeletal model and formulation.

## 2. Finite element model

### 2.1. Finite element modeling of the spine and trunk muscles

In this paper, a part of the human spine consisting of  $N$  vertebrae is considered. Each spinal motion segment consisting of vertebra-intervertebral disc-vertebra is modeled as a linear elastic beam element located at the vertebral body centers. Position vector of the  $i$ -th vertebral body center is given as a node by  $\mathbf{p}_i, i=1, 2, \dots, N$ . Assume that there are  $M_i$  muscles acting on  $i$ -th vertebra and  $\mathbf{F}_{i,j}^m, j=1, 2, \dots, M_i$ , denotes the  $j$ -th muscle force vector starting from the attachment point in  $i$ -th vertebra. We also assume that the muscle forces are generated statically to stabilize the spinal segment. Let  $\mathbf{p}_{i,j}$  be the position vector of the attachment point of  $j$ -th muscle acting on  $i$ -th vertebra. Geometric data such as vertebral positions and locations of muscle attachment points can be obtained from published anatomical data of the human spine and muscles (Stokes and Gardner-Morse, 1995; Stokes and Gardner-Morse, 1999).

### 2.2 Static equilibrium equations

Let us assume that the spinal system is in static equilibrium. The displacements including translations and rotations of each beam element are related with the forces and the moments acting on the vertebral body centers. Let us call these forces and moments motion segment forces and motion segment moments, respectively. The relation between the motion segment forces and the motion segment moments, and the displacements at vertebral nodes, could be defined as

$$\begin{bmatrix} \mathbf{F}_1^{ms} \\ \vdots \\ \mathbf{F}_N^{ms} \\ \mathbf{M}_1^{ms} \\ \vdots \\ \mathbf{M}_N^{ms} \end{bmatrix} = \mathbf{K} \cdot \begin{bmatrix} \mathbf{d}_1 \\ \mathbf{d}_2 \\ \vdots \\ \mathbf{d}_N \end{bmatrix} \quad (1)$$

where  $\mathbf{F}_i^{ms}$ ,  $\mathbf{M}_i^{ms}$ , and  $\mathbf{d}_i$ , denote the motion segment force, the motion segment moment, and the displacement vectors at  $i$ -th vertebral body center, respectively.  $\mathbf{K}$  represents the stiffness matrix describing linear elasticity of the spine model. The stiffness matrix  $\mathbf{K}$  of the motion segment can be experimentally obtained, as in Panjabi et al. (1976) and Gardner-Morse et al. (1990). The displacement vector  $\mathbf{d}_i$  at  $i$ -th node consists of the translation components,  $d_{i,k}^t, k=1,2,\dots,K$ , and the rotation components,  $d_{i,l}^r, l=1,2,\dots,L$ , where  $K$  and  $L$  are the number of translational and rotational degrees-of-freedom at each node, respectively.

Then, for given external forces  $\mathbf{F}_i^e$  and moments  $\mathbf{M}_i^e$  applied at  $i$ -th vertebral body center, the static equilibrium equations at the vertebral nodes can be formulated by

$$\sum_{j=1}^{M_i} \mathbf{F}_{i,j}^m - \mathbf{F}_i^{ms} + \mathbf{F}_i^e = \mathbf{0}, \quad i=1,2,\dots,N \quad (2)$$

$$\sum_{j=1}^{M_i} \mathbf{r}_{i,j} \times \mathbf{F}_{i,j}^m - \mathbf{M}_i^{ms} + \mathbf{M}_i^e = \mathbf{0}, \quad i=1,2,\dots,N \quad (3)$$

where  $\mathbf{r}_{i,j} = \mathbf{p}_i - \mathbf{p}_{i,j}$ , for all  $i$  and  $j$ , represents the moment arm of the muscle force.

### 2.3 The follower force and the shear force

It is necessary to discretize the follower force di-

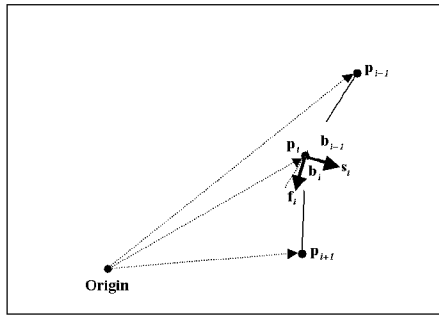
reaction at each node in order to decompose the resultant joint force into the follower force and the shear force. Let

$$\mathbf{b}_i = \frac{\mathbf{p}_{i+1} - \mathbf{p}_i}{\|\mathbf{p}_{i+1} - \mathbf{p}_i\|}, \quad i = 1, 2, \dots, N-1, \quad (4)$$

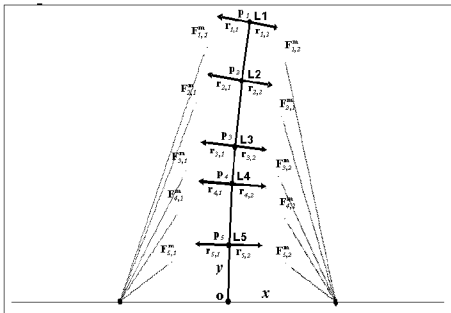
which indicates the direction of  $i$ -th beam element. Now let us define the follower force direction and the shear force direction at each vertebral body center (Fig. 1a). The follower force direction vector  $\mathbf{f}_i$  at  $i$ -th node is the mean direction of two adjacent beams and the shear force direction vector  $\mathbf{s}_i$  is perpendicular to the follower force direction formulated for  $i = 1, 2, \dots, N$ ,

$$\mathbf{f}_i = \frac{\mathbf{b}_{i-1} + \mathbf{b}_i}{\|\mathbf{b}_{i-1} + \mathbf{b}_i\|}, \quad (5)$$

$$\mathbf{f}_i \bullet \mathbf{s}_i = 0, \quad \|\mathbf{s}_i\| = 1, \quad (6)$$



(a)



(b)

Fig. 1. Two-dimensional finite element model of the lumbar spine and the psoas major muscles.

(a) Directions of follower force and shear force at  $i$ -th vertebral body center.

(b) Position vectors ( $\mathbf{p}_1 \sim \mathbf{p}_5$ ) of the five lumbar vertebral body centers and moment arm vectors ( $\mathbf{r}_{1,1} \sim \mathbf{r}_{3,2}$ ) and muscle force vectors ( $\mathbf{F}_{1,1}^m \sim \mathbf{F}_{5,2}^m$ ) at five vertebral body centers.

under the assumption that  $\mathbf{b}_0 = \mathbf{0}$ .

The resultant joint force at each vertebra is the sum of all the muscle forces, the applied external forces, and the compressive force transmitted from the upper vertebra. Hence, the resultant joint force,  $\mathbf{F}_i^j$ , at  $i$ -th vertebra is calculated iteratively: for  $i = 1, 2, \dots, N$ ,

$$\mathbf{F}_i^j = \sum_{j=1}^{M_i} \mathbf{F}_{1,j}^m + \mathbf{F}_i^e + \mathbf{F}_{i-1}^j = \mathbf{F}_i^{ms} + \mathbf{F}_{i-1}^j \quad (7)$$

with  $\mathbf{F}_0^j = \mathbf{0}$ .

Then,  $\mathbf{F}_i^j$  can be decomposed into the follower force  $\mathbf{F}_i^f$  and shear force  $\mathbf{F}_i^s$  at  $i$ -th node for  $i = 1, 2, \dots, N$ ,

$$\mathbf{F}_i^j = \mathbf{F}_i^f \oplus \mathbf{F}_i^s, \quad (8)$$

where  $\mathbf{F}_i^f // \mathbf{f}_i$  and  $\mathbf{F}_i^s // \mathbf{s}_i$ .

### 3. Optimization formulation

#### 3.1 Formulation of optimization problem under the follower force constraint

An optimization problem is formulated to investigate the muscle force distribution transmitting the resultant joint force along the follower force direction since the number of unknowns is larger than that of equations in Eq. (2) and Eq. (3). The sum of the magnitudes of follower forces at all vertebral body centers is regarded as an object function according to the assumption that the smaller follower force could generate less damage on intervertebral discs of the spine. Previous studies have supported this assumption that large compressive joint forces at the vertebra could accelerate chronic disk degeneration (White III and Panjabi, 1990). As constraint equations, the equilibrium equations, the follower force directions of the resultant joint forces, and the physiological bounds of the muscle forces and the vertebral displacements are applied. The final optimization problem can then be formulated as follows:

$$\text{Minimize } f = \sum_{i=1}^N \|\mathbf{F}_i^f\| \quad \text{s. t.} \quad (9)$$

Equilibrium constraint :

$$\mathbf{F}^m - \mathbf{K} \cdot \mathbf{d} + \mathbf{F}^e = \mathbf{0} \quad (10)$$

$$\text{where } \mathbf{F}^m = \begin{bmatrix} \sum_{j=1}^{M_1} \mathbf{F}_{1,j}^m \\ \vdots \\ \sum_{j=1}^{M_N} \mathbf{F}_{N,j}^m \\ \vdots \\ \sum_{j=1}^{M_1} \mathbf{r}_{1,j} \times \mathbf{F}_{1,j}^m \\ \vdots \\ \sum_{j=1}^{M_N} \mathbf{r}_{N,j} \times \mathbf{F}_{N,j}^m \end{bmatrix}, \mathbf{d} = \begin{bmatrix} \mathbf{d}_1 \\ \vdots \\ \vdots \\ \vdots \\ \mathbf{d}_N \end{bmatrix}, \mathbf{F}^e = \begin{bmatrix} \mathbf{F}_1^e \\ \vdots \\ \mathbf{F}_N^e \\ \mathbf{M}_1^e \\ \vdots \\ \mathbf{M}_N^e \end{bmatrix},$$

and  $\mathbf{K}$  is the stiffness matrix defined in Eq. (1)

*Follower force constraint :*

$$\|\mathbf{F}_i^s\| \leq \alpha \cdot F_{\max}^s, \quad i = 1, 2, \dots, N, \quad 0 \leq \alpha \leq 1 \quad (11)$$

where  $\alpha$  is a penalty parameter to restrict the shear force at all nodes and  $F_{\max}^s$  is the maximum value of the shear force generated when no muscle is activated for the given external loads. Small  $\alpha$  means a stricter follower force constraint.

*Physiological constraint :*

$$0 \leq \|\mathbf{F}_{i,j}^m\| \leq F_{i,j,\max}^m, \quad i = 1, 2, \dots, N, \quad j = 1, 2, \dots, M_i \quad (12)$$

where  $F_{i,j,\max}^m$  is the physiologically feasible upper bound of  $\mathbf{F}_{i,j}^m$ ,

$$0 \leq |d_{i,k}^t| \leq d_{i,k,\max}^t \quad \text{and} \quad 0 \leq |d_{i,l}^r| \leq d_{i,l,\max}^r, \quad i = 1, 2, \dots, N \quad (13)$$

where  $d_{i,k,\max}^t$  and  $d_{i,l,\max}^r$  denote the upper bounds of  $k$ -th translation component and of  $l$ -th rotation component of  $\mathbf{d}_i$ .

Theoretically, a pure follower force could be generated only when no shear force is allowed at each node, that is  $\alpha=0.0$ . However, a weak constraint Eq. (11) of the follower force was proposed in this study allowing shear force components of the joint force at all nodes in order to elucidate the relation between the follower force constraint and necessary muscle force distributions exerted.

### 3.2 Existence of the solution for the optimization problem

The general theorem regarding the existence of a

solution for the optimization problem is outlined below.

**Theorem** A constrained optimization problem given as follows

Minimize  $f(x)$  subject to  $x \in X$

where  $f : D \subset \mathbf{R}^n \rightarrow \mathbf{R}$  and  $X \subset D$ , has a solution in  $X$  if  $X$  is a non-empty, closed and bounded set and the objective function  $f$  is continuous on  $X$ .

Let us define a domain  $D_\alpha \subset \mathbf{R}^{dim}$  satisfying all the constraints, Eq. (10) - Eq. (13) with

$$dim = \sum_{i=1}^N \left\{ dimension(\mathbf{d}_i) + \sum_{j=1}^{M_i} dimension(\mathbf{F}_{i,j}^m) \right\} \quad (14)$$

It can be clearly proved that  $D_\alpha$  is closed and bounded, and the objective function  $f$  is continuous on  $D_\alpha$ . If  $D_\alpha$  is non-empty, then there exists a solution to the formulated optimization problem. Though it is not trivial that  $D_\alpha$  is non-empty for all  $\alpha$ , there must exist the largest integer  $t$ ,  $1 \leq t \leq S$ , such that  $D_{\alpha_t}$  is not empty for an arbitrary decreasing sequence  $\{\alpha_s\}_{s=1}^S$  with  $\alpha_1 = 1$  and  $\alpha_s = 0$  according to the attribute that  $D_\alpha \supset D_\beta$  if  $\alpha \geq \beta$  and  $D_1$  is not empty. If  $t = S$ , i.e.  $\alpha_t = 0$ , then it is shown that there is a muscle force distribution that could generate the joint forces transmit along the follower force direction without any shear force at the vertebral body centers.

## 4. Numerical tests

In this section, a two-dimensional problem of the lumbar spine (L1-S1) in the frontal plane is analyzed to confirm the developed finite element model and the formulation of the optimization problem investigating the activation of trunk muscles in the generation of follower forces at the vertebrae. Five node points were identified with the vertebral body centers of the lumbar spine, L1-L5, and five pairs of muscles were modeled based on the geometric data (Patwardhan et al., 2001; Stokes and Gardner-Morse, 1995; Stokes and Gardner-Morse, 1999) in a laterally flexed standing posture (Fig. 1b). A global coordinate system in the frontal plane was defined, with the origin at the center of the first sacral vertebra, the  $x$ -axis pointing horizontally to the right, and the  $y$ -axis pointing upward. The stiffness matrix  $\mathbf{K}$  was obtained from previous experimental literature (Panjabi et al., 1976; Gardner-Morse et al., 1990). The following values were necessary to solve the optimization problem:

Numbers of nodes and number of muscles at each node

$$N = 5, \quad M_1 = M_2 = M_3 = M_4 = M_5 = 2$$

Initial coordinates of nodes and muscle attachment points (Unit: mm)

The geometric data were given by Patwardhan et al. (2001), Stokes and Gardner-Morse (1995), and Stokes and Gardner-Morse (1999).

$$\begin{aligned} \mathbf{p}_1 &= (10.0, 190.0), \quad \mathbf{p}_2 = (6.2, 150.0), \\ \mathbf{p}_3 &= (3.1, 105.0), \quad \mathbf{p}_4 = (1.8, 80.0), \\ \mathbf{p}_5 &= (0.4, 38.0) \\ \|\mathbf{r}_{i,j}\| &= 15.0 \quad \text{and} \quad \mathbf{r}_{i,j} \perp \mathbf{b}_i, \quad i=1,2,\dots,N, \\ & \quad j=1, 2, \dots, M_i \end{aligned}$$

External forces and moments (Unit: N and Nm)

The external forces and moments used in this study represented 350 N of upper body weight with 3.5 Nm of lateral flexion.

$$\begin{aligned} \mathbf{F}_1^e &= (-350.0, 0.0), \quad \mathbf{F}_2^e = \mathbf{F}_3^e = \mathbf{F}_4^e = \mathbf{F}_5^e = (0.0, 0.0) \\ \mathbf{M}_1^e &= -3.5, \quad \mathbf{M}_2^e = \mathbf{M}_3^e = \mathbf{M}_4^e = \mathbf{M}_5^e = 0.0 \end{aligned}$$

Upper bounds of the shear force and muscle forces (Unit: N)

The maximum muscle forces activated are obtained from a previous study (Bogduk et al., 1992).

$$\begin{aligned} F_{\max}^s &= 82.5 \\ F_{i,j,\max}^m &= 300.0, \quad i=1,2,\dots,N, j=1, 2, \dots, M_i \end{aligned}$$

Upper bounds of the translation and rotation at each node (Unit: mm and degree)

$$\begin{aligned} d_{i,k,\max}^l &= 20.0 \quad \text{and} \quad d_{i,j,\max}^r = 10.0, \quad i=1,2,\dots,N, \\ k &= 1,2, \quad l=1 \end{aligned}$$

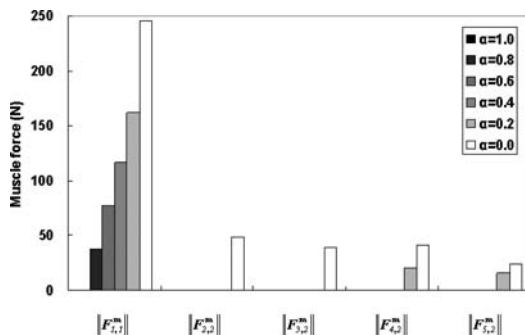


Fig. 2. Nonzero muscle forces at the five lumbar vertebrae for the variation of the penalty parameter  $\alpha$  under the follower force constraints.

The sequence of parameters

$$\{\alpha_s\}_{s=1}^S = \{1.0, 0.8, 0.6, 0.4, 0.2, 0.0\}, \quad S = 6$$

There was a muscle force distribution satisfying the formulated optimization problem on  $D_\alpha$  for  $\alpha = \alpha_s$  for all  $s = 1, \dots, S$ .  $\|\mathbf{F}_{1,2}^m\| = \|\mathbf{F}_{2,3}^m\| = \|\mathbf{F}_{3,1}^m\| = \|\mathbf{F}_{4,1}^m\| = \|\mathbf{F}_{5,1}^m\| = 0$  for all  $s = 1, \dots, S$  and the other muscle forces  $\|\mathbf{F}_{1,1}^m\|, \|\mathbf{F}_{2,2}^m\|, \|\mathbf{F}_{3,2}^m\|, \|\mathbf{F}_{4,2}^m\|$ , and  $\|\mathbf{F}_{5,2}^m\|$  are shown in Fig. 2. The magnitudes of muscle forces increased as  $\alpha$  decreased, and this implied the strict follower force constraint needed larger muscle forces to satisfy the follower force constraint. Only  $\mathbf{F}_{1,1}^m$  was nonzero when  $\alpha=0.8, 0.6$ , and  $0.4$ , while all the muscle forces were zero in the case of  $\alpha=1.0$ . This observation implied that little muscle forces were needed to satisfy the follower force constraint when a relatively large shear force was allowed at each vertebral body center. The activation of muscles was essential to make the directions of resultant joint forces approach the follower force directions. The follower force constraint may be related to spinal stability and the muscle force distribution may be related to the efficiency of energy or power; hence choosing a particular  $\alpha$  constitutes an individual's preference to obtain optimal status to maintain spinal stability.

At all vertebrae, the magnitude of follower force,  $\|\mathbf{F}_i^f\|$ , increased and that of shear force,  $\|\mathbf{F}_i^s\|$ , appro-

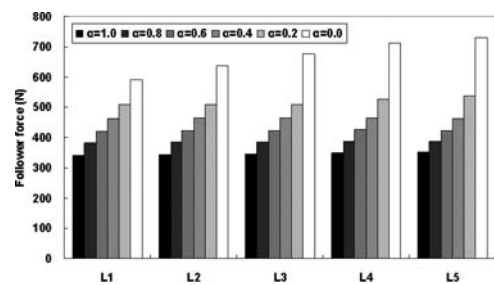


Fig. 3. Follower forces at the five lumbar vertebrae for the variation of the penalty parameter  $\alpha$ .

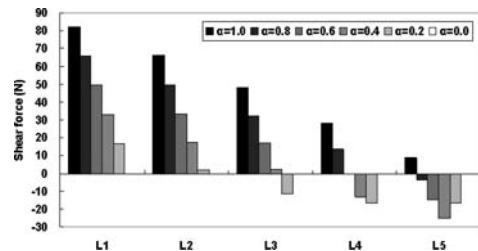


Fig. 4. Shear forces at the five lumbar vertebrae for the variation of the penalty parameter  $\alpha$ .

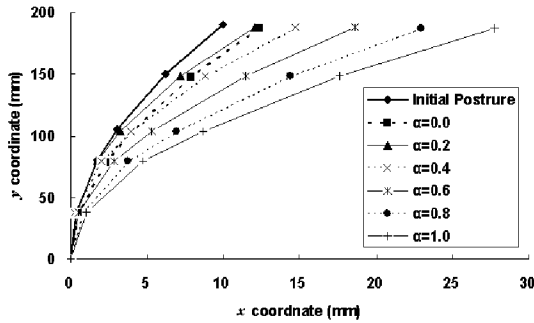


Fig. 5. Deformed shapes of the lumbar spine model for the variation of the penalty parameter  $\alpha$ .

ached zero while  $\alpha$  decreased (Fig. 3 and Fig. 4). When  $\alpha=0.0$ , the shear forces at all vertebrae were zero. These results indicated that the muscle forces calculated from the finite element model and optimization problem satisfied the given the follower force constraint perfectly. In other words, the resultant joint forces at all vertebral body centers became closer to the follower force direction as the parameter approached to zero.

Based on the calculated translations and rotations at the nodes, the deformed shapes of finite element model are shown in Fig. 5. A smaller  $\alpha$  value, which represented a stricter follower force constraint, generated a less deformed model shape. This phenomenon coincided with the previous experimental results that the translation and rotation of each vertebra were very small under relatively great external loads if the compressive load was transmitted along the follower load direction (Patwardhan et al., 1999; Patwardhan et al., 2000; Patwardhan et al., 2001). In addition, the results showed that muscle force distributions contributed to preserving spinal stability by generating the necessary resultant joint forces approaching the follower force directions.

### 5. Conclusions

A finite element model with a subsequent optimization problem of the musculoskeletal system in the human spine was formulated in order to investigate the relation between the follower force concept and spinal stability and the role of muscle force activation to the spinal stability. A two-dimensional test problem dealing with the lumbar spine and the trunk muscles was numerically solved to validate the developed model. The results showed that the necessary muscle force distributions could be obtained

to minimize the compressive joint force, satisfying the follower force constraint. A stronger follower force constraint increases the compressive joint forces and muscle forces, and decreases deformation of the spinal model, thus increasing spinal stability. The results indicate that the role of follower force in spinal stability coincides with the findings of clinical and experimental studies and the muscle force distribution contributes to generating the necessary joint forces for spinal stability. By expanding the model to three-dimension and implementing more muscles with realistic anatomic data, the developed finite element model and optimization formulation will provide a quantitative investigation of the trunk muscles on spinal stability under follower forces.

### Acknowledgement

This work was supported by the Korea Research Foundation Grant funded by the Korean Government (MOEHRD) (KRF-2005-003-D00492).

### Nomenclature

- $\alpha$  : Penalty parameter to restrict the shear force at all nodes
- $\mathbf{b}_i$  : Direction of  $i$ -th beam element
- $\mathbf{d}_i$  : Displacement vector at  $i$ -th vertebral body center
- $d_{i,j}^r$  : Rotation components of  $\mathbf{d}_i$ ,  $l=1,2,\dots,L$
- $d_{i,j,\max}^r$  : Upper bound of  $l$ -th rotation component of  $\mathbf{d}_i$
- $d_{i,k}^t$  : Translation components of  $\mathbf{d}_i$ ,  $k=1, 2, \dots, K$
- $d_{i,k,\max}^t$  : Upper bound of  $k$ -th translation component of  $\mathbf{d}_i$
- $\mathbf{f}_i$  : Follower force direction vector at  $i$ -th node
- $\mathbf{F}_i^e$  : Given external force applied at  $i$ -th vertebral body center
- $\mathbf{F}_i^f$  : Follower force at  $i$ -th node
- $\mathbf{F}_i^j$  : Resultant joint force at  $i$ -th vertebra
- $\mathbf{F}_{i,j}^m$  :  $j$ -th muscle force vector starting from the attachment point in  $i$ -th vertebra
- $F_{i,j,\max}^m$  : Physiologically feasible upper bound of  $\mathbf{F}_{i,j}^m$
- $\mathbf{F}_i^{\text{ms}}$  : Motion segment force at  $i$ -th vertebral body center
- $\mathbf{F}_i^s$  : Shear force at  $i$ -th node
- $F_{\max}^s$  : Maximum value of the shear force

generated when no muscle is activated for the given external load

- K** : Stiffness matrix describing linear elasticity of the spine model
- $M_i$  : Number of muscles acting on  $i$ -th vertebra
- $M_i^c$  : Given external moment applied at  $i$ -th vertebral body center
- $M_i^{ms}$  : Motion segment moment at  $i$ -th vertebral body center
- $N$  : Number of modeled vertebrae
- $p_i$  : Position vector of the  $i$ -th vertebral body center,  $i=1, 2, \dots, N$
- $p_{i,j}$  : Position vector of the attachment point of  $j$ -th muscle acting on  $i$ -th vertebra
- $r_{i,j}$  : Moment arm of the muscle force for  $i$  and  $j$
- $s_i$  : Shear force direction vector at  $i$ -th node

## References

- Beck, M., 1952, "Die Knicklast Des Einseitig Einge-Spannten, Tangential Gedrückten Stabes," *Zeitschrift für Angewandte Mathematik und Physik (ZAMP)*, Vol. 3, pp. 225~228 and 476~477.
- Bogduk, N., Macintosh, J. E., Percy, M. J., 1992, "A Universal Model of the Lumbar Back Muscles in the Upright Position," *Spine* Vol. 17, pp. 897~913.
- Gardner-Morse, M. G., Laible, J. P., Stokes, I. A. F., 1990, "Incorporation of Spinal Flexibility Measurements into Finite Element Analysis," *Journal of Biomechanical Engineering* Vol. 112, pp. 481~483.
- Langthjem, M. A., Sugiyama, Y., 2000, "Dynamic Stability of Columns Subjected to Follower Loads: A Survey," *Journal of Sound and Vibration* Vol. 238, pp. 809~851.
- Leipholtz, H., 1980, *Stability of Elastic Systems*, Sijthoff & Noordhoff.
- Panjabi, M. M., Brand Jr., R. A., White III, A. A., 1976, "Three-Dimensional Flexibility and Stiffness Properties of the Human Thoracic Spine," *Journal of Biomechanics* Vol. 9, pp. 185~192.
- Patwardhan, A. G., Havey, R. M., Meade, K. P., Lee, B., Dunlap, B., 1999, "A Follower Load Increases the Load-Carrying Capacity of the Lumbar Spine in Compression," *Spine* Vol. 24, pp. 1003~1009.
- Patwardhan, A. G., Havey, R. M., Ghanayem, A. J., Diener, H., Meade, K. P., Dunlap, B., Hodges, S. D., 2000, "Load-Carrying Capacity of the Human Cervical Spine in Compression is Increased Under a Follower Load," *Spine* Vol. 25, pp. 1548~1554.
- Patwardhan, A. G., Meade, K. P., Lee, B., 2001, "A Frontal Plane Model of the Lumbar Spine Subjected to a Follower Load: Implications for the Role of Muscles," *Journal of Biomechanical Engineering* Vol. 123, pp. 212~217.
- Pflüger, A., 1955, "Zur Stabilität Des Tangential Gedrückten Stabes," *Zeitschrift für Angewandte Mathe-matik und Mechanik(ZAMM)* Vol. 35, pp. 191.
- Rohlmann, A., Neller, S., Claes, L., Bergman, G., Wilke, H. -J., 2001, "Influence of a Follower Load on Intradiscal Pressure and Intersegmental Rotation of the Lumbar Spine," *Spine* Vol. 26, pp. E557~E561.
- Ryu, B. J., Katayama, K., Sugiyama, Y., 1998, "Dynamic Stability of Timoshenko Columns Subjected to Subtangential Forces," *Computers and Structures* Vol. 68, pp. 499~512.
- Stokes, I. A. F., Gardner-Morse, M. G., 1995, "Lumbar Spine Maximum Efforts and Muscle Recruitment Patterns Predicted by a Model with Multijoint Muscles and Joints with Stiffness," *Journal of Bio-mechanics* Vol. 28, pp. 173~186.
- Stokes, I. A. F., Gardner-Morse, M. G., 1999, "Quantitative Anatomy of the Lumbar Musculature," *Journal of Biomechanics* Vol. 32, pp. 311~316.
- Wang, Q., 2003, "On Complex Flutter and Buckling Analysis of a Beam Structure Subjected to Static Follower Force," *Structural Engineering and Mechanics* Vol. 16, pp. 533~556.
- White III, A. A., Panjabi, M. M., 1990, *Clinical Biomechanics of the Spine, 2nd edition*, Lippincott Williams & Wilkins.